

Astrophysical and theoretical physics implications from multimessenger neutron star observations

Hector O. Silva,¹ A. Miguel Holgado,^{2,3} Alejandro Cárdenas-Avenidaño,^{4,1} and Nicolás Yunes¹

¹*Department of Physics, University of Illinois at Urbana-Champaign, Urbana, Illinois 61801, USA*

²*Department of Astronomy, University of Illinois at Urbana-Champaign, Urbana, Illinois 61801, USA*

³*National Center for Supercomputing Applications, University of Illinois at Urbana-Champaign, Urbana, Illinois 61801, USA*

⁴*Programa de Matemática, Fundación Universitaria Konrad Lorenz, 110231 Bogotá, Colombia*

The *Neutron Star Interior Composition Explorer* (NICER) recently measured the mass and equatorial radius of the isolated neutron star PSR J0030+0451. We use these measurements to infer the moment of inertia, the quadrupole moment, and the surface eccentricity of an isolated neutron star for the first time, using relations between these quantities that are insensitive to the unknown equation of state of supranuclear matter. We also use these results to forecast the moment of inertia of neutron star *A* in the double pulsar binary J0737-3039, a quantity anticipated to be directly measured in the coming decade with radio observations. Combining this information with the measurement of the tidal Love number with LIGO/Virgo observations, we propose and implement the first theory-agnostic and equation-of-state-insensitive test of general relativity. Specializing these constraints to a particular modified theory, we find that consistency with general relativity places the most stringent constraint on gravitational parity violation to date, surpassing all other previously reported bounds by seven orders of magnitude.

Neutron stars are some of the most extreme objects in Nature. Their mass (typically around $1.4M_{\odot}$) combined with their small radius (between 10–14 km) result in interior densities that can exceed nuclear saturation density ($\rho \geq 2.8 \times 10^{14}$ g/cm³), above which exotic states of matter can arise [1]. Neutron stars are, next to black holes, the strongest gravitational field sources known, with typical gravitational potentials that are five-orders of magnitude larger than that of the Sun. These properties make neutron stars outstanding laboratories to study both matter and gravity in situations out of reach in terrestrial and Solar System experiments.

Our current poor understanding of the supranuclear equation of state translates, via the equations of stellar equilibrium, to a large variability on observable properties of neutron stars, such as their masses and radii [2]. This variability increases if one lifts the assumption that Einstein’s theory of general relativity is valid in the strong-gravity environment of neutron star interiors [3]. Modifications to general relativity generically predict new equations of stellar equilibrium, which, when combined with uncertainties on the nuclear equation of state, jeopardize attempts to test Einstein’s theory with isolated, neutron star observations.

One possibility to circumvent this issue is to explore whether relations between neutron-star observables that are insensitive to either (or both) the equation of state and the gravitational theory exist. Fortunately, they do. For instance, when properly nondimensionalized, the moment of inertia (I), the rotational quadrupole moment (Q) and the tidal Love number (λ) of neutron stars show a remarkable degree of equation-of-state insensitivity, at a level below 1% [4, 5]. These “I-Love-Q” relations also exist in some modified theories of gravity, although they are different from their general relativity counterparts [6].

We here combine the first measurements [7, 8] by NICER [9] of *both* the mass (M) and equatorial radius (R_e) of the isolated pulsar PSR J0030+0451 [10, 11] with equation-of-state insensitive relations involving the compactness ($\mathcal{C} = GM/(R_e c^2)$) to infer a number of astrophysical and theoretical physics consequences. Before doing so, let us explain how

these relations are obtained.

Approximately universal relations. Neutron stars can have short rotation periods of the order of milliseconds, so their surfaces are oblate instead of spherical. The inclusion of this effect is of critical importance to accurately model the thermal X-ray waveform that NICER observes, since the X-rays are produced by hotspots at the star’s surface [12, 13]. The canonical approach to model relativistic rotating stars was developed in the 1970s [14, 15]. In this approach, the star’s rotation is treated as a small perturbation $\varepsilon = f/f_0 \ll 1$, involving the star’s rotation frequency f and its characteristic mass-shedding frequency $f_0 = (GM/R_e^3)^{1/2}/(2\pi)$. Rotating stars are then found by perturbing in ε an otherwise non-rotating star, which can be obtained by solving the Tolman-Oppenheimer-Volkoff equations [16]. This slow-rotation approximation is well-justified for most neutron stars with astrophysically relevant spins. Even for a prototypical millisecond pulsar with $f = 700$ Hz, $M = 1.4M_{\odot}$ and $R_e = 11$ km, one has $\varepsilon = 0.37$. In the case of PSR J0030+0451, its rotation frequency is known to be $f_{\star} = 205.53$ Hz [10, 11], so $\varepsilon_{\star} = 0.14$, when one uses the best-fit M and R_e values obtained by NICER [7, 8]. Henceforth, a “★” indicates observables associated with PSR J0030+0451.

Using this technique, we numerically calculated over a thousand neutron star solutions to order ε^2 in this perturbative scheme, using a broad set of 46 different equations of state [17, 18], as detailed in the Methods section. From these solutions, we then numerically computed the moment of inertia I , the rotational quadrupole moment Q , the surface eccentricity e , and the electric-type, $\ell = 2$, tidal Love number λ , which is the dominant parameter in the description of tidal effects in the late inspiral of neutron star binaries [19–21]. We nondimensionalized these quantities through division by the appropriate factors of M and dimensionless spin $\chi = (2\pi f_0)G\bar{I}M/c^3$, namely: $\bar{I} = c^4 I/(G^2 M^3)$, $\bar{Q} = -c^4 Q/(G^2 M^3 \chi^2)$ and $\bar{\lambda} = \lambda/M^5$. The relations between these nondimensional quantities are strongly insensitive to the equation of state.

The first step in using the approximately universal relations

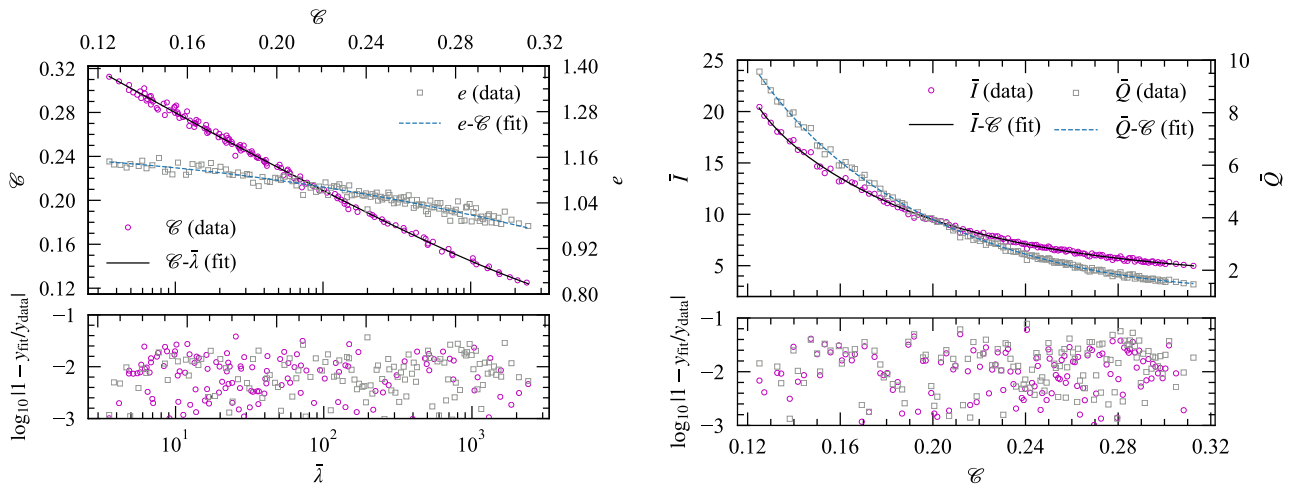


FIG. 1. The \mathcal{C} -relations. The top-left panel shows the relation between tidal Love number $\bar{\lambda}$ and compactness \mathcal{C} (bottom and left axes) and between eccentricity e and compactness \mathcal{C} (top and right axes). The top-right panel shows the relation between the moment of inertia \bar{I} (left axes), rotational quadrupole moment \bar{Q} (right axes) and compactness \mathcal{C} . The lower panels show the relative errors ($\epsilon = |1 - y_{\text{fit}}/y_{\text{data}}|$) between the data and the fits. The largest mean relative error among the four \mathcal{C} relations is 2% (corresponding to the Q - \mathcal{C} relation), which shows the equation-of-state insensitivity of the relations.

on NICER’s first observation is to derive equation-of-state-insensitive relations between the observables $\{\bar{I}, \bar{Q}, \bar{\lambda}, e\}$, with respect to the compactness \mathcal{C} . Figure 1 shows these “ \mathcal{C} -relations”, which exhibits a weak dependence on the equation of state; details on the fits are given in the Methods section. Our plan of attack is then clear: use the publicly available Markov-Chain Monte Carlo (MCMC) M - R_c samples [22] for the best-fit, three-hotspot model inferred by the Illinois-Maryland analysis of the NICER data [8] to obtain a posterior distribution for the compactness [22], and then use the approximately universal relations to infer other astrophysical quantities. We detail this procedure next.

Astrophysical implications. We begin by constructing a posterior distribution $P(\mathcal{C}|\text{NICER})$ for the compactness \mathcal{C} of PSR J0030+0451, using the MCMC chains [22]. With this posterior in hand, we then use the \mathcal{C} -relations to infer posterior distributions for $\{\bar{I}, \bar{\lambda}, \bar{Q}, e\}$.

The implementation of such an inference procedure requires a particular scheme, and we here follow a proposal that accounts for the approximately universal nature of the relations [18]. In this scheme, the maximum relative error of each fitting function defines the half-width of the 90% credible interval of a Gaussian distribution centered at each fitted value. The posterior distribution for each dimensionless quantity is then calculated using the corresponding \mathcal{C} -relation and the posterior distribution of the compactness, after marginalizing over the latter. From these posteriors and using the same procedure described above, we can also construct posteriors for the dimensionful versions of these quantities by a change of variables, marginalize over the nuisance variables mass M and radius R_c , and then do a final rescaling of the posterior by ϵ ($= 0.14$) for the surface eccentricity e and by ϵ^2 for the rotational quadrupole moment Q . This process is detailed in the Methods section.

Parameter	Median	-1σ	$+1\sigma$	-2σ	$+2\sigma$
\bar{I}_\star (10)	1.31	1.20	1.45	1.11	1.61
$\bar{\lambda}_\star$ (10^2)	4.97	3.68	6.90	2.80	9.76
\bar{Q}_\star	5.92	5.31	6.64	4.79	7.46
I_\star (10^{45} g cm 2)	1.71	1.22	2.34	0.87	3.06
Q_\star (10^{43} g cm 2)	1.49	1.04	2.12	0.73	2.89
e_\star (10^{-1})	1.56	1.36	1.82	1.19	2.05

TABLE I. Inferred properties of PSR J0030+0451 using equation-of-state-insensitive relations. We report the values within one and two standard deviations from the mean, representing about 68% and 95% confidence intervals, respectively. These values are the first inferences of the moment of inertia, the eccentricity, the Love number and the quadrupole moment of an isolated neutron star.

The resulting median, 1σ and 2σ intervals of these parameters (both the nondimensionalized and the dimensionful versions) are shown in Table I; see the Methods section for plots of the inferred posteriors. The reported confidence intervals in all of these quantities account for both the approximate nature of the universal relations and the uncertainties in NICER’s observation. These results are the *first inferences on the moment of inertia, the surface eccentricity, the Love number and the quadrupole moment of an isolated neutron star*.

We can also use NICER’s observation combined with the I - \mathcal{C} relation to estimate the moment of inertia of PSR J0737-3039A ($I_{1.3381}$), where the subscript refers to this pulsar’s measured mass of $M = (1.3381 \pm 0.0007) M_\odot$ [23]. The double pulsar J0737-3039 is expected to provide the first direct neutron star measurement of the moment of inertia [24]. This system is the only double-pulsar observed to date, which makes it an unique laboratory for binary stellar astrophysics [25, 26]. Moreover, an accurate measurement of $I_{1.3381}$ in combination

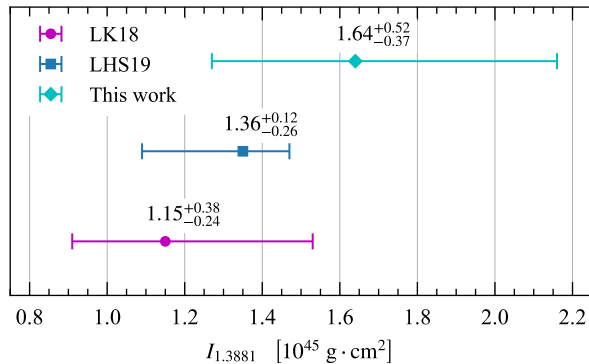


FIG. 2. Predictions for the moment of inertia of PSR J0737-3039A. We compare our prediction $I_{1.3381}$ against: (i) Landry and Kumar [28] (“LK18”), which used binary Love [32] and I-Love relations with the tidal-deformability constraints from binary neutron-star merger GW170817 [30], and (ii) Lim et al. [29] (“LHS19”) which carried out Bayesian modeling of a number of equations of state.

with its known mass is expected to strongly constrain the nuclear equation of state around once and twice nuclear saturation density [27].

To predict the moment of inertia of PSR J0737-3039A from NICER’s observation of PSR J0030+0451, we first need to obtain an estimate for the compactness $\mathcal{C}_{1.3381}$ of PSR J0737-3039A. This can be approximated by the substitution $\{M, R_e\} \mapsto \{M_0 = 1.3381 M_\odot, R_e\}$ at each MCMC sample [22] and then computing \mathcal{C}_{M_0} . This yields an approximation to the distribution of compactness for a system with mass M_0 , which is assumed known and identical to PSR J0030+0451. This procedure is only justified as long as M_0 is very close to M_\star , as in the case of PSR J0737-3039A, whose inferred mass ($M_0 = 1.3381^{+0.0007}_{-0.0007} M_\odot$) [23] is within the 1σ credible interval of NICER’s mass inference ($M_\star = 1.44^{+0.15}_{-0.14} M_\odot$) [8].

With an estimate of the compactness of PSR J0737-3039A, we can now obtain a prediction for PSR J0030+0451’s moment of inertia repeating the procedure applied to PSR J0030+0451. Figure 2 shows our result, $I_{1.3381} = 1.64^{+0.52}_{-0.37} \times 10^{45} \text{ g cm}^2$, together with two other independent predictions [28, 29]. The anticipated future independent measurement of $I_{1.3381}$ from continued radio timing of PSR J0737-3039A will provide another test for nuclear theory and enable an ‘I-Love test’ of gravity, the latter of which we define next.

Theoretical physics implications. The combination of the inference of I with NICER data described above, and the independent measurement of λ [30] by the LIGO/Virgo collaboration from the binary neutron-star merger GW170817 [31], allows for the first implementation of an I-Love test [4]. This test would be the first *multi-messenger test of general relativity with neutron star observables*.

The idea of an I-Love test is as follows [4, 5] (see Fig. 3). Consider two independent inferences of $\bar{I}_{1.4}$ and $\bar{\lambda}_{1.4}$ for a $1.4 M_\odot$ neutron star. In the $(\bar{I}, \bar{\lambda})$ -plane, these measurements yield a 90% confidence error box. If the I-Love relation in general relativity, including its small equation-of-state vari-

ability, *does not* pass through this error box, then there is evidence for a violation of Einstein’s theory, regardless of the underlying equation of state. Moreover, if any theory of gravity predicts an I-Love curve that also does not pass through this error box for a given value of its coupling constants, then the I-Love test places a constraint on the couplings of this theory, which is also independent of the equation of state.

Such a test, however, requires the inference of the tidal deformability and the moment of inertia of a neutron star of the *same* mass. The LIGO/Virgo collaboration used gravitational wave data to infer the tidal deformability of a $1.4 M_\odot$ neutron star to be $\bar{\lambda}_{1.4} = 190^{+390}_{-120}$ at 90% confidence [33], obtained under the assumptions that the binary components were described by the same equation of state and were slowly-spinning. We can use NICER data to infer the moment of inertia of a $1.4 M_\odot$ neutron star with the same techniques we used to predict the moment of inertia of PSR J0737-3039A. This gives $\mathcal{C}_{1.4} = 0.159^{+0.025}_{-0.022}$ and $\bar{I}_{1.4} = 14.6^{+4.5}_{-3.3}$ at 90% confidence. An important underlying assumption behind both inferences is that general relativity is the correct theory of gravity.

Since carrying out such a test on a theory-by-theory basis would in general be complicated and time-consuming, we here develop and implement a useful *parametrization* of the I-Love test. From Newtonian gravity, we know that \bar{I} scales with \mathcal{C}^{-2} , whereas $\bar{\lambda}$ scales with \mathcal{C}^{-5} . Therefore, $\bar{I} = C_{\bar{I}\bar{\lambda}} \bar{\lambda}^{2/5}$, with $C_{\bar{I}\bar{\lambda}} \approx 0.52$ a constant that depends on the equation of state very weakly [5]. This calculation can be extended, systematically, in a *post-Minkowskian expansion*, i.e., an expansion in powers of $\mathcal{C} \ll 1$ [34]. The outcome is that both \bar{I} and $\bar{\lambda}$ can be written as a power series in \mathcal{C} and then be combined (as just described in the Newtonian limit) to obtain $\bar{I} = \bar{I}(\bar{\lambda})$. The resulting I-Love relation has the same degree of equation-of-state independence as the original I-Love relation [4]. For our neutron star catalog, a parameterization in general relativity of the form

$$\bar{I}_{\text{GR}} = \bar{\lambda}^{2/5} (c_0 + c_1 \bar{\lambda}^{-1/5} + c_2 \bar{\lambda}^{-2/5}), \quad (1)$$

with $c_0 = 0.584$, $c_1 = 0.980$, $c_2 = 2.695$, is sufficient to reproduce our numerical data with mean relative error $\langle \epsilon^{\bar{I}} \rangle \leq 2 \times 10^{-3}$. The prefactor $\bar{\lambda}^{2/5}$ is the Newtonian result, while the powers of $\bar{\lambda}^{-1/5}$ inside parenthesis are relativistic (post-Minkowskian) corrections because $\bar{\lambda}^{-1/5} \propto \mathcal{C} \lesssim 0.2$. Given this, we then propose a minimal deformation of the Einsteinian parameterization in Eq. (1) of the form

$$\bar{I}_{\text{p}} = \bar{I}_{\text{GR}} + \beta \bar{\lambda}^{-b/5}, \quad \beta \in \mathbb{R}_+, \quad b \in \mathbb{Z}, \quad (2)$$

where β and b are deformation parameters that control the magnitude and type of the deviations from general relativity in the I-Love relation respectively. Such a parameterization is similar to that successfully used in gravitational-wave tests of general relativity by the LIGO/Virgo collaboration, the parameterized post-Einsteinian framework [35].

We performed such a test of general relativity through the procedure described earlier. First, we see that the I-Love relation in general relativity does indeed pass this null-test and it is consistent with the error box. Second, we considered

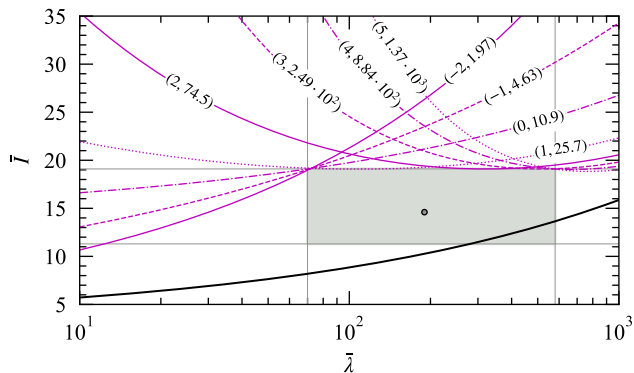


FIG. 3. Multimessenger test of general relativity using the parametrized I-Love relation. The vertical (horizontal) lines delimit the 90% confidence region (shaded) for $\bar{\lambda}_{1,4}$ [33] ($\bar{I}_{1,4}$, this work), while the circle marks the median (190, 14.6). The solid black line corresponds to the I-Love relation in general relativity [Eq. (1)] and is consistent with the inferred values of $\bar{I}_{1,4}$, $\bar{\lambda}_{1,4}$ at 90% confidence. Starting from $b = -2$ and moving clockwise, we show the parametrized I-Love curves (b, β_{crit}), where $b \in [-2, 5]$ and β_{crit} is the critical value of β above which the parametrized I-Love relation [Eq. (2)] fails to pass by the 90% confidence region in the plane.

$b \in [-2, 5]$, where the lower limit is set by requiring no deviations at the Newtonian level and the upper limit is set for simplicity. We then fixed b and calculated what the corresponding value of $\beta = \beta_{\text{crit}}$ is, above which the parametrized I-Love relation (2) would be in tension with the inferred ($\bar{I}_{1,4}$, $\bar{\lambda}_{1,4}$) region at 90% confidence. Our results are summarized in Fig. 3, where the numbers in parenthesis correspond to (b, β_{crit}) . We stress that our results for $b \leq 0$ are of course dependent on the posterior used for $\bar{\lambda}_{1,4}$. If one treated the tidal deformabilities as independent free parameters in the waveform model [31], then the $\bar{\lambda}_{1,4}$ posterior would not have a lower limit, allowing all curves with $b \leq 0$ to be consistent with both observations.

With these theory-agnostic constraints in hand, we can now map them to specific theories and place constraints on their coupling parameters. As an example, let us consider dynamical Chern-Simons gravity, a theory that modifies general relativity by introducing gravitational parity-violation [36]. Mathematical well-posedness requires the theory to be treated as an effective field theory [37]. In this formalism, one works in a small-coupling approximation $\zeta \equiv 16\pi\alpha^2\mathcal{R}^{-4} \ll 1$, where $\mathcal{R} = [c^2R_c^3/(GM)]^{1/2}$ is the curvature length scale associated with a neutron star (in our case), and where α is a coupling constant with units of length squared, such that ζ is dimensionless. This theory modifies Einstein's only when gravity is strong, and thus, it passes all Solar System constraints, being only extremely-weakly constrained by Gravity Probe B and the LAGEOS satellites, and table-top experiments, to $\alpha^{1/2} \leq 10^8$ km [38, 39]. This theory has also evaded gravitational-wave tests [40], making it a key target to test the constraining power of our new I-Love test.

Let us now map the theory-agnostic deformation of the I-Love relations in Eq. (2) to dynamical Chern-Simons gravity, though this methodology could be applied to other theories

as well. As we discuss in the Methods section, the I-Love relation in this theory can be described by Eq. (2) with $b_{\text{CS}} = 4$ and $\beta_{\text{CS}} = 6.15 \times 10^{-2} \bar{\xi}$, where $\bar{\xi} = 16\pi\alpha^2/M^4$. We can now use our theory-agnostic constraints on β to place a constraint on α , the coupling constant of dynamical Chern-Simons gravity. Using the constraint on β when $b = 4$, namely $\beta_{\text{crit}} \leq 8.84 \times 10^2$, and applying the mapping, yields $\beta_{\text{CS}} = 6.15 \times 10^{-2} \bar{\xi} \leq 8.84 \times 10^2$, or simply

$$\alpha^{1/2} \leq 8.5 \text{ km}, \quad (3)$$

at 90% credibility, if the theory is to be consistent with inferences of $\bar{I}_{1,4}$ and $\bar{\lambda}_{1,4}$ assuming general relativity. Using the mean value $\mathcal{C}_{1,4} = 0.159$, which implies the mean equatorial radius $R_{1,4} = 13.0$ km, we also find that $\zeta \leq 0.23$ when using Eq. (3), implying that the small-coupling approximation is indeed satisfied. This bound is *seven-orders of magnitude stronger than any previous constraints [38], and it is unlikely to be improved upon with foreseeable gravitational-wave observations [41]*.

Conclusions and outlook. The NICER observation of PSR J0030+0451 allows the extraction of new astrophysical and theoretical physics inferences when one uses equation-of-state-insensitive relations. We have here derived the first measurements of the moment of inertia, the quadrupole moment, the surface eccentricity and the Love number of an isolated neutron star. We have also been able to perform the first theory-agnostic and equation-of-state independent test of general relativity by combining NICER and LIGO/Virgo observations. This test, in turn, was leveraged to produce the most stringent constraint on gravitational parity violation, improving previous bounds by seven orders of magnitude. This robust methodology can be applied to future multi-messenger observations of neutron stars with NICER and gravitational wave observatories, with important implications to nuclear astrophysics and theoretical physics.

Acknowledgments. We thank Toral Gupta, Fred Lamb, Philippe Landry and Helvi Witek for discussions. We thank also Cole Miller, Sharon Morsink and Kent Yagi for suggestions that improved this work. We thank the NICER collaboration for making [8] publicly available. H.O.S, A.C.-A. and N.Y. are supported by NASA Grants No. NNX16AB98G, 80NSSC17M0041 and 80NSSC18K1352 and NSF Award No. 1759615. A.C.-A. also acknowledges funding from the Fundaci3n Universitaria Konrad Lorenz (Project 5INV1). A.M.H. is supported by the DOE NNSA Stewardship Science Graduate Fellowship under Grant No. DE-NA0003864.

– Methods –

Equation of state catalog. We consider the large catalog of nuclear equations of state of [18], supplemented by the non-duplicates from [17]. To this set of 85 equations of state, we impose the following observational consistency criteria. First, the equation of state must be consistent with the 90% confidence region of the 2-dimensional marginalized posterior (M , R_c) reported by the LIGO/Virgo collaboration [33] for each component of the binary neutron-star merger GW170817.

Second, the equation of state must be consistent with the 90% confidence region of the 2-dimensional marginalized posterior (M , R_e) reported by NICER [8] for PSR J0030+0451. Third, the equation of state must allow for neutron stars with masses above $M_{\max} \geq 1.96 M_\odot$, which corresponds to the lower-limit estimate of the most massive neutron star known, the millisecond pulsar J0740+6620, at 95.4% confidence level [42]. In total, this yields the following 46 equations of state: ALF2, APR3, APR4, BCPM BSP, BSR2, BSR2Y, BSk20, BSk21, BSk22, BSk23, BSk24, BSk25, BSk26, DD2, DD2Y, DDHd, DDME2, DDME2Y, ENG, FSUGarnet, G3, GNH3, IOPB, K255, KDE0v1, MPA1, Model1, Rs, SINPA, SK272, SKOp, SKa, SKb, SLY2, SLY230a, SLY4, SLY9, SLy, SkI2, SkI3, SkI4, SkI6, SkMP, WFF1 and WFF2 [17, 18].

Our numerical code to calculate neutron stars (in general relativity and dynamical Chern-Simons gravity) uses the piecewise-polytrope approximation to model these equations of state [17]. In this approximation, the relationship between pressure (p_i) and baryonic mass density (ρ_i) is given by $p_i = K_i \rho_i^{\Gamma_i}$, where K_i is the polytropic index and Γ_i the adiabatic index, on a sequence of baryonic mass density intervals i . For the high-baryonic mass densities describing the neutron star core ($\rho_{\text{core}} \gtrsim 1.7 \times 10^{14} \text{ g/cm}^{-3}$, the exact value depends on the equation of state) we used a three-segment approximant, fitted to the equation of states listed above. For low-baryonic mass densities ($\rho < \rho_{\text{core}}$), matter is described using a four-segment approximant fitted against the SLy equation of state [17, 18].

One could argue [43] that a more rigorous approach to do inference on the nuclear equation of state from neutron star observations is to not use hard cuts as we do here. However, since our approach makes use of equation-of-state independent relations, changes to our equation of state catalog imply only small changes to the numerical values of the fitting coefficients. The hard cuts then have a negligible impact on our inferences, since the uncertainty on our quoted results (e.g., in Table I) are dominated by the uncertainties on the observations, except for the eccentricity e_* .

Neutron-star catalog. For each equation of state, we calculate a sequence of 50 neutron stars, spanning central baryonic mass densities in the range $\rho_c \in [1.5, 8.0] \rho_{\text{nuc}}$ (where $\rho_{\text{nuc}} = 2.8 \times 10^{14} \text{ g/cm}^{-3}$ is the nuclear saturation density) in general relativity and in dynamical Chern-Simons gravity. To obtain neutron star solutions in dynamical Chern-Simons gravity we use the same perturbative expansion in small-spin ($\varepsilon \ll 1$) as used in general relativity, outlined in the main text, but combined with a small-coupling ($\zeta \ll 1$) approximation as required for the well-posedness of the theory [44]. We then retained only those with (i) $M \leq M_{\max}$ (i.e. linearly stable against radial perturbations) and (ii) with $\mathcal{C} \in [0.125, 0.3125]$ (i.e. within the prior on \mathcal{C} used in the parameter estimation of PSR J0030+0451 by the Illinois-Maryland NICER team [8]). In the case of dynamical Chern-Simons gravity only we further imposed (iii) that all stars have $\zeta \leq 0.2$ (the small-coupling approximation).

\mathcal{C} -relations. The equation-of-state insensitive \mathcal{C} -relations

are of the form

$$y = \sum_{i=0}^n a_i x^i, \quad (4)$$

and are shown in Fig. 1. The values of the coefficients a_i , the number of coefficients n , and the mean $\langle e^y \rangle$ and maximum relative error $\epsilon_{\max}^y = \max |1 - y/y_{\text{fit}}|$ of the resulting fits are presented in Table II.

Parameter inference – PSR J0030+0451. To calculate the posterior distributions for $y = \{\bar{I}, \bar{\lambda}, \bar{Q}, e\}$, we follow the procedure used in [18]. In this scheme, the maximum relative error ϵ_{\max}^y (cf. the last column of Table II) is used to define the half-width of the 90% credible interval of a Gaussian distribution centered at each fitted value (y_{fit}),

$$P(y|\mathcal{C}) = (2\pi\sigma_y^2)^{-1/2} \exp\left[-(y - y_{\text{fit}})^2 / (2\sigma_y^2)\right], \quad (5)$$

where $\sigma_y = \epsilon_{\max}^y y_{\text{fit}} / 1.645$.

The posterior distribution for each dimensionless quantity, $P(y|\text{NICER})$, is then calculated using the corresponding \mathcal{C} -relation and the posterior probability distribution of the compactness, $P(\mathcal{C}|\text{NICER})$ (see Fig. 4), obtained directly using the Illinois-Maryland NICER samples [22], and then marginalizing over \mathcal{C} :

$$P(y|\text{NICER}) = \int P(y|\mathcal{C}) P(\mathcal{C}|\text{NICER}) d\mathcal{C}. \quad (6)$$

What dominates the uncertainty on our inferred values for the neutron star parameters? Is it the uncertainties associated with the \mathcal{C} -measurement we are using, or those introduced by the approximate universality of the \mathcal{C} -relations? To answer this question, in Figure 5 we show the resulting posterior distributions by taking into account the approximate universality of the \mathcal{C} -relations (solid lines) and compare against the posterior distributions on the same parameters if we do not (dashed lines). In the latter case, the posteriors are obtained by directly applying the M - R_e samples [22] in the \mathcal{C} -relations. The effect of including the systematic error induced by the variability of the \mathcal{C} -relations is to broaden the posterior, a small effect for \bar{I} , $\bar{\lambda}$ and \bar{Q} , but not for the eccentricity e . The reason is the following: the mean relative error for the e - \mathcal{C} fit is approximately 4%, which is larger than the variability of e in the 1σ interval of its distribution. This leads to the considerable broadening shown in the bottom-right panel of Fig. 5.

The posteriors for the dimensionful version of these quantities are obtained of through a change of variables, and using the posteriors on M and R_e . For instance, for the moment of inertia I ,

$$P(I|\text{NICER}) = (c^2/G)^2 \int P(c^4 I / (G^2 M^3) | \text{NICER}) \times P(M | \text{NICER}) M^{-3} dM. \quad (7)$$

The posterior distributions for the dimensionful variables are similar in shape to their nondimensionalized versions.

Parameter inference – fixed mass. To calculate the posterior distribution of a quantity y for a neutron star with known

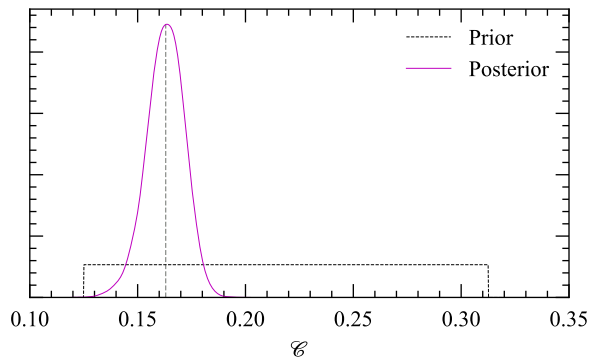


FIG. 4. Prior and posterior probability distributions on the compactness of PSR J0030+0451 (\mathcal{C}_*). The Illinois-Maryland analysis [8, 22] assumed a flat prior probability distribution for \mathcal{C}_* with bounds 0.125 and 0.3125 (dashed curve). The posterior probability distribution (solid line) has a median value of $\mathcal{C}_* = 0.163$ [8]. The posterior is approximately Gaussian and very different from the flat (uninformative) prior used by NICER, showing that the NICER observation was indeed informative.

mass M_0 using the \mathcal{C} -relations, we first need to construct a posterior $P(\mathcal{C}_{M_0}|\text{NICER})$ given $P(\mathcal{C}|\text{NICER})$. To do so, we write

$$P(\mathcal{C}_{M_0}|\text{NICER}) = P([GM/(R_e c^2)]_{M=M_0}|\text{NICER}), \quad (8)$$

where the right-hand side is obtained by using the MCMC samples [22], doing the substitution $\{M, R_e\} \mapsto \{M_0, R_e\}$ at each sample and then computing \mathcal{C}_{M_0} . This procedure gives an approximation to the distribution of compactness for a system with known mass M_0 , which we here take to be identical to PSR J0030+0451. Of course, the posterior \mathcal{C}_{M_0} obtained in this way would fail dramatically if the difference between M_0 and PSR J0030+0451's mass, $M_* = 1.44^{+0.15}_{-0.14} M_\odot$ [8], is large. However, this is not case for a canonical neutron star with mass $1.4 M_\odot$ and PSR J0737-3039A's, which has a mass of $1.3381 M_\odot$ masses, both of which agree with M_* within 1σ .

Knowing $P(\mathcal{C}_{M_0}|\text{NICER})$, we can use it in Eq. (6) and marginalize over \mathcal{C}_{M_0} to obtain the posterior distribution of a quantity y at mass M_0 . Our results for \mathcal{C} , R_e and $y = \{\bar{I}, \bar{\lambda}, \bar{Q}, e\}$ for a canonical neutron star are summarized in Table III.

I-Love relation in dynamical Chern-Simon gravity. Let us describe further how to map the theory-agnostic deformation of the I-Love relations in Eq. (2) to dynamical Chern-Simons gravity. The procedure outlined here can be applied to other theories as well.

The dimensionless moment of inertia of a constant density star in dynamical Chern-Simons gravity is $\bar{I} = \bar{I}_{\text{GR}} + \bar{I}_{\text{CS,N}}$, where $\bar{I}_{\text{CS,N}} = C_{\bar{I}}^{\text{CS,N}} \alpha^2 M/R^5$ and $C_{\bar{I}}^{\text{CS,N}} = 1024\pi/75$ [45] to leading-order in α and leading-order in \mathcal{C} . The I-Love relations in dynamical Chern-Simons gravity are insensitive to the equation of state when \bar{I}_{CS} is normalized via $\bar{\xi} \equiv 16\pi\alpha^2/M^4$ [46]. Therefore, using that $\bar{\lambda}_{\text{N}} = (1/2)\mathcal{C}^{-5}$ in Newtonian gravity for a constant density star, we then have that $\bar{I}_{\text{CS,N}} = (16\pi)^{-1} C_{\bar{I}}^{\text{CS,N}} \bar{\xi} \mathcal{C}^5 = [(32\pi)^{-1} C_{\bar{I}}^{\text{CS,N}} \bar{\xi}] \bar{\lambda}^{-1}$. Although this relation was derived assuming a constant density star, it holds for any equation of state, with variability at the sub-percent

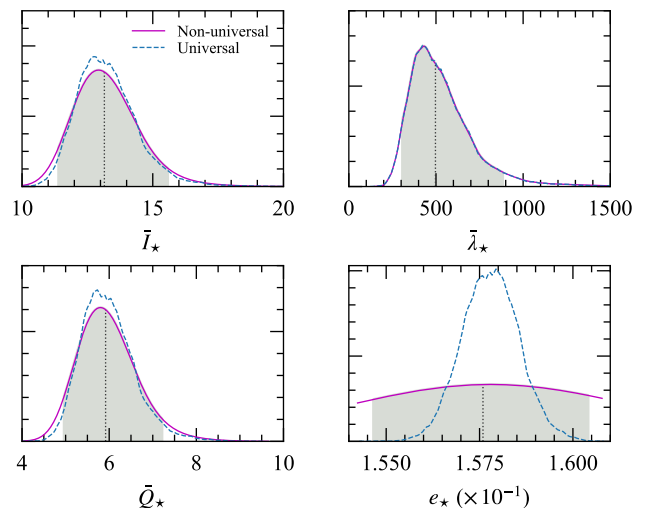


FIG. 5. Posterior distributions on the dimensionless quantities $\{\bar{I}, \bar{\lambda}, \bar{Q}, e\}$ of PSR J0030+0451. We show both the distributions obtained by taking into account the systematic error introduced by the approximate universality of the \mathcal{C} -relations (solid lines) and that assuming the universality of the relations (dashed lines). The vertical lines and the shaded bands represent the mean and 90% posterior credible intervals, respectively. The posteriors show that for \bar{I} , $\bar{\lambda}$ and \bar{Q} , the uncertainties associated with our inferences are dominated by the uncertainty on the measured value \mathcal{C}_* . This is not the case for e , because the systematic error associated with the e - \mathcal{C} fit is larger than that associated with the inference of e , assuming complete equation-of-state independence on the e - \mathcal{C} relation.

level [46]. Comparison of this result to Eq. (2) reveals that the mapping between our proposed parameterization and dynamical Chern-Simons gravity is $\beta_{\text{CS,N}} = (32/75)\bar{\xi}$ and $b_{\text{CS,N}} = 5$.

How well does this “Newtonian” approximation capture the fully relativistic I-Love relation in dynamical Chern-Simons gravity? Figure 6 shows that the Newtonian approximation derived above is excellent for low-mass neutron stars. The scaling with $\bar{\lambda}^{-1}$, however, fails for more massive stars, when $M \gtrsim 1 M_\odot$, because relativistic corrections become important. In spite of this, the dynamical Chern-Simons correction to the relativistic I-Love data, for values of $\bar{\lambda}$ corresponding to stars with compactness \mathcal{C} within NICER's priors, can be well-approximated by $\bar{I}_{\text{CS}} = \beta_{\text{CS}} \bar{\lambda}^{-b_{\text{CS}}/5}$, with

$$\beta_{\text{CS}} = 6.15 \times 10^{-2} \bar{\xi}, \quad b_{\text{CS}} = 4. \quad (9)$$

This functional form is quite close to the Newtonian result (in fact, just a factor of \mathcal{C} higher than the Newtonian result because $\mathcal{C} \propto \bar{\lambda}^{-1/5}$), which suggests the rule of thumb $b = b^{\text{N}} - 1$, where b^{N} is the result of the I-Love calculation to Newtonian order in modified gravity.

By virtue of the parity properties of the field equations in dynamical Chern-Simons gravity, the electric-type $\ell = 2$ tidal Love number in this theory is identical to that in general relativity, for slowly-rotating neutron stars.

Why can neutron stars constrain dynamical Chern-Simons gravity? Let us do a back-of-the-envelope estimate to

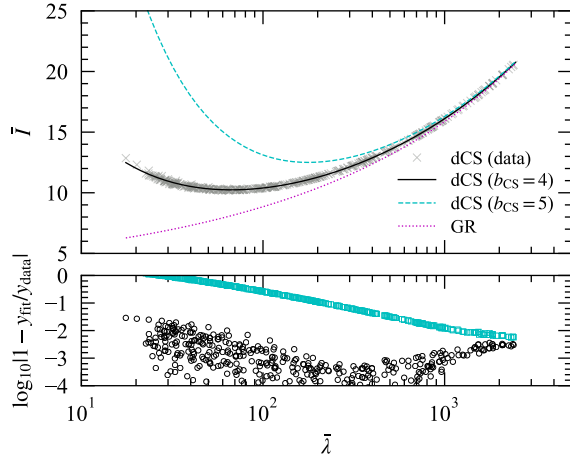


FIG. 6. I-Love relation in dynamical Chern-Simons gravity. In the top-panel we show the numerical data (crosses) obtained for neutron stars in dynamical Chern-Simons, the I-Love relation in general relativity (dotted line) and fits to it using the Newtonian result obtained in the main text (dashed line) and the post-Minkowskian corrected result (solid line). In the bottom-panel we show the relative errors between both fits and the data, explicitly showing that the Newtonian fit cannot be used for an I-Love test. In this figure we fixed $\bar{\xi} = 10^3$ and only show stars with $\zeta \leq 0.25$.

y	x	n	a_0	a_1	a_2	a_3	a_4	$\langle \epsilon^y \rangle$	ϵ_{\max}^y
$\log \bar{I}_{\text{GR}}$	\mathcal{C}^{-1}	4	5.56×10^{-1}	-1.77×10^{-1}	1.11×10^{-1}	-1.51×10^{-2}	6.94×10^{-4}	1.52×10^{-2}	6.7×10^{-2}
\mathcal{C}	$\log \bar{\lambda}_{\text{GR}}$	4	3.59×10^{-1}	-8.81×10^{-2}	1.31×10^{-2}	-4.58×10^{-3}	6.99×10^{-4}	9.63×10^{-3}	4.2×10^{-2}
$\log \bar{Q}_{\text{GR}}$	\mathcal{C}	4	2.11	-1.47×10^1	6.69×10^1	-2.11×10^2	2.66×10^2	1.91×10^{-2}	8.6×10^{-2}
e	\mathcal{C}	2	1.16	2.05×10^{-1}	-2.59	-	-	9.86×10^{-3}	4.1×10^{-2}

TABLE II. Numerical coefficients for the fits to the \mathcal{C} -relations. These fits are tailored to the Illinois-Maryland MCMC data samples [22] and, therefore, are only valid within the compactness range $\mathcal{C} \in [0.125, 0.3125]$.

Parameter	Source / Universal relation	Median	-1.65σ	$+1.65\sigma$
$\mathcal{C}_{1.4} (10^{-1})$	MCMC chain / -	1.59	1.37	1.84
$R_{1.4} (10) [\text{km}]$	MCMC chain / -	1.30	1.12	1.51
$\bar{I}_{1.4} (10)$	MCMC chain / I- \mathcal{C}	1.46	1.12	1.91
$\bar{\lambda}_{1.4} (10^2)$	MCMC chain / Love- \mathcal{C}	5.80	2.33	13.7
$\bar{Q}_{1.4}$	MCMC chain / Q- \mathcal{C}	6.12	4.52	8.12
$e_{1.4,0}$	MCMC chain / e- \mathcal{C}	1.12	1.09	1.15

TABLE III. Properties of $M = 1.4 M_{\odot}$ neutron stars, inferred from PSR J0030+0451 at 90% credibility. The eccentricity $e_{1.4,0}$ is evaluated at the characteristic mass-shedding frequency f_0 . To rescaled it to the eccentricity $e_{1.4}$ of a star spinning with frequency f one has to multiply by $\varepsilon = f/f_0 = 1532.7 \text{ Hz}$.

b	-2	-1	0	1	2	3	4	5
β_{crit}	1.97	4.63	10.8	25.7	74.5	2.49×10^2	8.84×10^2	3.15×10^3

TABLE IV. Constraints on the parametrized I-Love relation. For a given exponent b , parametrized I-Love curves with $\beta \geq \beta_{\text{crit}}$ do not pass through the 90% credible intervals on the inferred values of $\bar{I}_{1.4}$ and $\bar{\lambda}_{1.4}$ as shown in Fig. 3.

explain *why* neutron star observations have such a constraining power in dynamical Chern-Simons gravity. Assume that ζ has been constrained to some value, say $\zeta \leq 0.25$, by some set of observations that involve also measurements of the mass and equatorial radius of a neutron star. A posterior distribution for $\alpha^{1/2}$ can then be obtained by translating the MCMC samples for M and R_e into samples of $\alpha^{1/2} = [\zeta/(16\pi)]^{1/4} \mathcal{R}$. Using for concreteness the MCMC samples obtained by NICER, one would obtain $\alpha^{1/2} \leq 8.57^{+0.93}_{-1.13} \text{ km}$ (at 90% credibility), which is very close to the real constraint derived in the main text. The back-of-the-envelope estimate presented above is of course *not an actual constraint since NICER alone cannot bound ζ due to degeneracies with the equation of state*. But this estimate does tell us that such a test would be dominated by \mathcal{R} , because an improvement on the bound on ζ by a factor of k would only improve the constraint on $\alpha^{1/2}$ by $k^{1/4}$.

– Tables –

- [1] G. Baym, T. Hatsuda, T. Kojo, P. D. Powell, Y. Song, and T. Takatsuka, “From hadrons to quarks in neutron stars: a review,” *Rept. Prog. Phys.* **81**, 056902 (2018).
- [2] F. Özel and P. Freire, “Masses, Radii, and the Equation of State of Neutron Stars,” *Ann. Rev. Astron. Astrophys.* **54**, 401–440 (2016).
- [3] E. Berti *et al.*, “Testing General Relativity with Present and Future Astrophysical Observations,” *Class. Quant. Grav.* **32**, 243001 (2015).
- [4] K. Yagi and N. Yunes, “I-Love-Q,” *Science* **341**, 365–368 (2013).
- [5] K. Yagi and N. Yunes, “I-Love-Q Relations in Neutron Stars and their Applications to Astrophysics, Gravitational Waves and Fundamental Physics,” *Phys. Rev. D* **88**, 023009 (2013).
- [6] D. D. Doneva and G. Pappas, “Universal Relations and Alternative Gravity Theories,” *Astrophys. Space Sci. Libr.* **457**, 737–806 (2018).
- [7] T. E. Riley *et al.*, “A NICER View of PSR J0030+0451: Millisecond Pulsar Parameter Estimation,” *Astrophys. J. Lett.* **887**, L21 (2019).
- [8] M. C. Miller *et al.*, “PSR J0030+0451 Mass and Radius from NICER Data and Implications for the Properties of Neutron Star Matter,” *Astrophys. J. Lett.* **887**, L24 (2019).
- [9] K. C. Gendreau *et al.*, “The Neutron star Interior Composition Explorer (NICER): design and development,” in *Proc. SPIE, Society of Photo-Optical Instrumentation Engineers (SPIE) Conference Series*, Vol. 9905 (2016) p. 99051H.
- [10] A. N. Lommen, A. Zepka, D. C. Backer, M. McLaughlin, J. C. Cordes, Z. Arzoumanian, and K. Xilouris, “New pulsars from an Arecibo drift scan search,” *Astrophys. J.* **545**, 1007 (2000).
- [11] Z. Arzoumanian *et al.* (NANOGrav), “The NANOGrav 11-year Data Set: High-precision timing of 45 Millisecond Pulsars,” *Astrophys. J. Suppl.* **235**, 37 (2018).
- [12] S. M. Morsink, D. A. Leahy, C. Cadeau, and J. Braga, “The Oblate Schwarzschild Approximation for Light Curves of Rapidly Rotating Neutron Stars,” *Astrophys. J.* **663**, 1244–1251 (2007).
- [13] S. Bogdanov *et al.*, “Constraining the Neutron Star Mass–Radius Relation and Dense Matter Equation of State with NICER. II. Emission from Hot Spots on a Rapidly Rotating Neutron Star,” *Astrophys. J.* **887**, L26 (2019).
- [14] J. B. Hartle, “Slowly rotating relativistic stars. 1. Equations of structure,” *Astrophys. J.* **150**, 1005–1029 (1967).
- [15] J. B. Hartle and K. S. Thorne, “Slowly Rotating Relativistic Stars. II. Models for Neutron Stars and Supermassive Stars,” *Astrophys. J.* **153**, 807 (1968).
- [16] S. L. Shapiro and S. A. Teukolsky, *Black holes, white dwarfs, and neutron stars: The physics of compact objects* (1983).
- [17] J. S. Read, B. D. Lackey, B. J. Owen, and J. L. Friedman, “Constraints on a phenomenologically parameterized neutron-star equation of state,” *Phys. Rev. D* **79**, 124032 (2009).
- [18] B. Kumar and P. Landry, “Inferring neutron star properties from GW170817 with universal relations,” *Phys. Rev. D* **99**, 123026 (2019).
- [19] T. Mora and C. M. Will, “Numerically generated quasiequilibrium orbits of black holes: Circular or eccentric?” *Phys. Rev. D* **66**, 101501 (2002).
- [20] E. E. Flanagan and T. Hinderer, “Constraining neutron star tidal Love numbers with gravitational wave detectors,” *Phys. Rev. D* **77**, 021502 (2008).
- [21] T. Hinderer, “Tidal Love numbers of neutron stars,” *Astrophys. J.* **677**, 1216–1220 (2008).
- [22] M. C. Miller *et al.*, “NICER PSR J0030+0451 Illinois-Maryland MCMC Samples,” (2019).
- [23] M. Kramer *et al.*, “Tests of general relativity from timing the double pulsar,” *Science* **314**, 97–102 (2006), arXiv:astro-ph/0609417 [astro-ph].
- [24] M. Kramer and N. Wex, “The double pulsar system: A unique laboratory for gravity,” *Class. Quant. Grav.* **26**, 073001 (2009).
- [25] I. H. Stairs, S. E. Thorsett, R. J. Dewey, M. Kramer, and C. A. McPhee, “The Formation of the Double Pulsar PSR J0737-3039A/B,” *Mon. Not. Roy. Astron. Soc.* **373**, L50–L54 (2006).
- [26] R. D. Ferdman *et al.*, “The double pulsar: evidence for neutron star formation without an iron core-collapse supernova,” *Astrophys. J.* **767**, 85 (2013).
- [27] J. M. Lattimer and B. F. Schutz, “Constraining the equation of state with moment of inertia measurements,” *Astrophys. J.* **629**, 979–984 (2005).
- [28] P. Landry and B. Kumar, “Constraints on the moment of inertia of PSR J0737-3039A from GW170817,” *Astrophys. J.* **868**, L22 (2018).
- [29] Y. Lim, J. W. Holt, and R. J. Stahulak, “Predicting the moment of inertia of pulsar J0737-3039A from Bayesian modeling of the nuclear equation of state,” *Phys. Rev. C* **100**, 035802 (2019).
- [30] B. P. Abbott *et al.* (LIGO Scientific, Virgo), “Properties of the binary neutron star merger GW170817,” *Phys. Rev. X* **9**, 011001 (2019).
- [31] B. P. Abbott *et al.* (LIGO Scientific, Virgo), “GW170817: Observation of Gravitational Waves from a Binary Neutron Star Inspiral,” *Phys. Rev. Lett.* **119**, 161101 (2017).
- [32] K. Yagi and N. Yunes, “Binary Love Relations,” *Class. Quant. Grav.* **33**, 13LT01 (2016).
- [33] B. P. Abbott *et al.* (LIGO Scientific, Virgo), “GW170817: Measurements of neutron star radii and equation of state,” *Phys. Rev. Lett.* **121**, 161101 (2018).
- [34] T. K. Chan, A. P. O. Chan, and P. T. Leung, “I-Love relations for incompressible stars and realistic stars,” *Phys. Rev. D* **91**, 044017 (2015).
- [35] N. Yunes and F. Pretorius, “Fundamental Theoretical Bias in Gravitational Wave Astrophysics and the Parameterized Post-Einsteinian Framework,” *Phys. Rev. D* **80**, 122003 (2009).
- [36] R. Jackiw and S. Y. Pi, “Chern-Simons modification of general relativity,” *Phys. Rev. D* **68**, 104012 (2003), gr-qc/0308071.
- [37] T. Delsate, D. Hilditch, and H. Witek, “Initial value formulation of dynamical Chern-Simons gravity,” *Phys. Rev. D* **91**, 024027 (2015).
- [38] S. Alexander and N. Yunes, “Chern-Simons Modified General Relativity,” *Phys. Rept.* **480**, 1–55 (2009).
- [39] K. Yagi, N. Yunes, and T. Tanaka, “Slowly Rotating Black Holes in Dynamical Chern-Simons Gravity: Deformation Quadratic in the Spin,” *Phys. Rev. D* **86**, 044037 (2012), [Erratum: Phys. Rev. D 89, 049902 (2014)].
- [40] R. Nair, S. Perkins, H. O. Silva, and N. Yunes, “Fundamental Physics Implications for Higher-Curvature Theories from Binary Black Hole Signals in the LIGO-Virgo Catalog GWTC-1,” *Phys. Rev. Lett.* **123**, 191101 (2019).
- [41] S. H. Alexander and N. Yunes, “Gravitational wave probes of parity violation in compact binary coalescences,” *Phys. Rev. D* **97**, 064033 (2018).
- [42] H. T. Cromartie *et al.*, “Relativistic Shapiro delay measurements of an extremely massive millisecond pulsar,” *Nat. Astron.* **4**, 72–76 (2019).

- [43] M. C. Miller, C. Chirenti, and F. K. Lamb, “Constraining the Equation of State of High-density Cold Matter Using Nuclear and Astronomical Measurements,” *Astrophys. J.* **888**, 12 (2020).
- [44] K. Yagi, L. C. Stein, N. Yunes, and T. Tanaka, “Isolated and Binary Neutron Stars in Dynamical Chern-Simons Gravity,” *Phys. Rev. D* **87**, 084058 (2013), [Erratum: *Phys. Rev. D* **93**, no. 8, 089909 (2016)].
- [45] Y. Ali-Haïmoud and Y. Chen, “Slowly-rotating stars and black holes in dynamical Chern-Simons gravity,” *Phys. Rev. D* **84**, 124033 (2011).
- [46] T. Gupta, B. Majumder, K. Yagi, and N. Yunes, “I-Love-Q Relations for Neutron Stars in dynamical Chern Simons Gravity,” *Class. Quant. Grav.* **35**, 025009 (2018).